

THE FREE-ELECTRON LASER VARIABLE BRIDGE COUPLER*

G. Spalek, J. H. Billen, J. A. Garcia, P. M. Giles,
L. D. Hansborough, D. E. McMurry, and S. B. Stevens,[†] AT-1, MS H817

Los Alamos National Laboratory, Los Alamos, NM 87545

Summary

The Los Alamos free-electron laser (FEL) is being modified to test a scheme for recovering most of the power in the residual 20-MeV electron beam by decelerating the microbunches in a linear standing-wave accelerator and using the recovered energy to accelerate new beam. A variable-coupler low-power model that resonantly couples the accelerator and decelerator structures has been built and tested. By mixing the TE₁₀₁ and TE₁₀₂ modes, this device permits continuous variation of the decelerator fields relative to the accelerator fields through a range of 1:1 to 1:2.5. Phase differences between the two structures are kept below 1° and are independent of power-flow direction. The rf power is also fed to the two structures through this coupling device. Measurements were also made on a three-post-loaded variable coupler that is a promising candidate for the same task.

Introduction

A schematic of the Los Alamos FEL energy recovery experiment (ERX)¹ is shown in Fig. 1. The beam will be accelerated by two side-coupled linear accelerators and, after passage through the FEL, some of the beam energy will be recovered by decelerating the beam in similar LINAC structures. Variable couplers will do the following:

- Feed recovered beam energy from the decelerators to the accelerators
- Lock the phases of the acceleration and deceleration fields to each other
- Couple the structures to the power sources through a coupler-to-waveguide iris
- Vary the ratio of accelerator-to-decelerator fields through a range of ~1:1 to ~2:1 (that is, vary the amount of energy recovered from the beam).

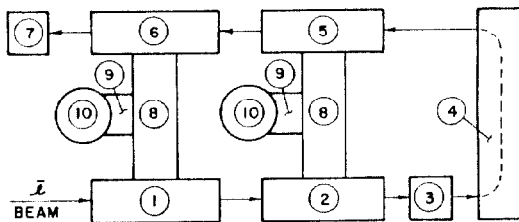


Fig. 1. ERX: (1) 13-cell accelerator, (2) 15-cell decelerator, (3) FEL, (4) beam transport, (5) 15-cell decelerator, (6) 13-cell decelerator, (7) beam dump, (8) variable couplers, (9) waveguides, and (10) power sources.

The accelerator beam-loading factor will be

$$n = \frac{P_b}{P_b + P_{cav}} = 0.74$$

*Work performed for Strategic Defense Initiatives Office and Ballistic Missile Defense Advanced Technology Center under auspices of US Dept. of Energy.

[†]Now at the University of Illinois, Urbana, Illinois.

P_b = beam power, and P_{cav} = cavity power.

This paper reports the results of tests made on a low-power coupler model that meets the requirements and on another coupler that is a good candidate for the same task.

Description of Variable Coupler

A schematic diagram of the variable coupler chosen and tested is shown in Fig. 2. The coupler consists of a center cell (coupled to the waveguide through an iris) and two resonant coupling cells. The coupling cells are designed to bolt onto the standard waveguide flanges at the midpoints of the accelerators (existing) and decelerators (now being fabricated).

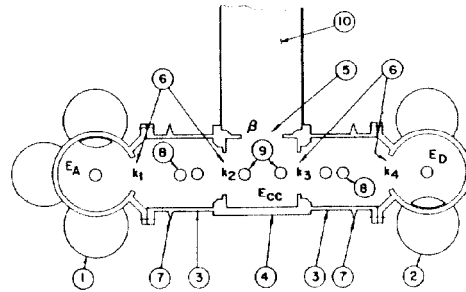


Fig. 2. Variable coupler: (1) accelerator, (2) decelerator, (3) coupling cells, (4) coupler center cell, (5) iris, (6) coupling slots, (7) expansion joint, (8) fixed post tuners, (9) movable post tuners, and (10) power waveguide.

Coupling factors between the structures and coupler resonators are k_1 , k_2 , k_3 , and k_4 (Fig. 2). The fields of the accelerator, decelerator, and coupler center cell are given by E_A , E_D , and E_{CC} , respectively. For the structure $\pi/2$ mode, the ratios of these fields are given by

$$\frac{E_A}{E_D} = \left(\frac{k_4}{k_3} \right) \left(\frac{k_2}{k_1} \right), \quad \frac{E_A}{E_{CC}} = \frac{k_2}{k_1}, \quad \text{and} \quad \frac{E_D}{E_{CC}} = \frac{k_3}{k_4}$$

Coupling factors k_1 and k_4 are equal in the ERX but not in the low-power tests, as will be described later. The ratio E_A/E_D is varied by varying the ratio k_2/k_3 in the coupler. To do this, the coupler center cell is loaded with two off-center tuning posts. When these posts are inserted to equal depths, only the TE₁₀₁ mode is excited at the 1.3-GHz operating frequency. Unequal post insertion, while keeping the resonant frequency constant, mixes the TE₁₀₁ and TE₁₀₂ modes of the center cell. The relative phases of these modes are 0° or 180°, depending on which tuning post is inserted deeper into the center cell. The admixture of modes leads to an asymmetry of the cavity fields and, therefore, to a difference in the effective coefficients k_2 and k_3 .

To keep the high-power coupler's center-cell fields below 1.5 Kilpatrick, the coupling cells were also loaded with off-center posts to make k_1 , k_2 , k_3 , and k_4 approximately equal when maximum beam energy is being recovered (that is, when $E_A \approx E_D$).

Measurements, Scaling, and Results

The FEL accelerator cavities were not available for testing of the low-power coupler model. Instead, the accelerator and decelerator were replaced by existing 8- and 5-cell accelerator structures, respectively, which were of similar design. Measurements made using these cavities were scaled to the final cavities and results checked when the latter became available.

The measurement sequence was as follows:

- Coupler was isolated; center-cell tuners inserted to equal depth (that is $k_2 = k_3$); k_2 and k_3 were extracted from the coupler mode-spectrum.
- Perturbation measurements were made with entire system coupled to determine relative field strengths in each structure as the center-cell tuner positions were varied. Coupling constants k_1 , k_4 , and relative stored energies per cell (U) were extracted from data.
- Relative phases of the fields in the 8- and 5-cell structures were measured as the rf drive was moved to different parts of the system and the tuner positions varied.
- The Q of the 8-cell structure was degraded by a factor of $\sqrt{2}$, and the relative phases re-measured.
- The waveguide coupling factor (β_C) and unloaded Q of the coupled system (Q_C) were measured.
- The waveguide coupling factor (β_5) of the 5-cell structure was measured.
- The Q of the coupler center cell (Q_{CC}) was measured with the coupling cell slots taped over with aluminum tape giving an underestimate of Q_{CC} .

Figure 3 shows the field ratios (E_8/E_5) obtained versus the position of one of the center-cell tuners, the other tuner being set to keep the resonant frequency of the $\pi/2$ mode at 1.3 GHz. The range of field ratios E_8/E_5 was 1:1 to 2.5:1. Figure 4 shows the corresponding relative phases of the fields as the system was driven from different points. Also shown are the phases when the system was driven from the 5-cell structure and when the 8-cell structure was detuned by 150 kHz. This gives an idea of the sensitivity to tuning of the coupled system.

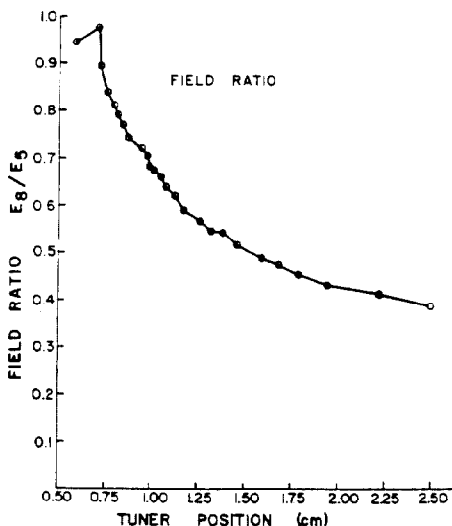


Fig. 3. Accelerator-to-decelerator field ratio.

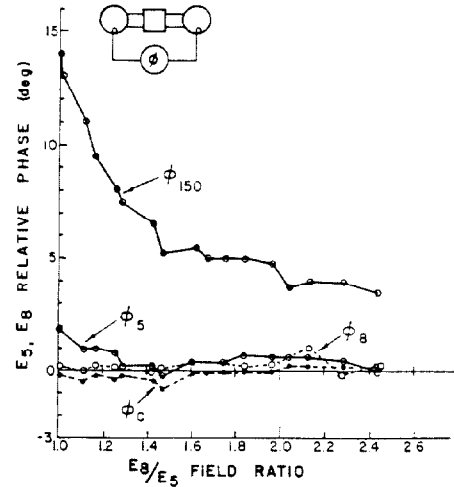


Fig. 4. Accelerator to decelerator phase variation versus field ratio: ϕ_5 - drive in 5-cell structure; ϕ_8 - drive in 8-cell structure; ϕ_C - drive in center cell; ϕ_{150} - drive in 5-cell structure, 8-cell structure detuned by 150 kHz.

All phases remained unchanged when the Q of the 8-cell structure was lowered by a factor of $\sqrt{2}$.

Values of parameters measured for equal center-cell tuner lengths were

$$\begin{aligned} k_1 &= 0.015 & \beta_5 &= 5.5 & Q_{CC} &= 419 \\ k_2 &= k_3 = 0.0299 & \beta_C &= 2.07 & U_{CC} &= 0.0224 \\ k_4 &= 0.0197 & Q_C &= 5580 & U_5 &= 0.0521 \\ & & U_8 &= 0.0874 & & \end{aligned}$$

The quantities U_5 , U_{CC} , and U_8 are the respective stored energies (per cell) of the 5-cell, coupler center cell, and 8-cell structures, relative to the total stored energy.

These parameter values were used to scale the system to one having the accelerator and decelerator replaced by the existing FEL 15- and 13-cell structures. Corresponding waveguide coupling factors are $\beta_{15} = 3.5$ and $\beta_{13} = 2.8$, and Q values are equal to the 5-cell structure's Q , which is $\sim 21,000$. If the primed quantities represent the scaled values, then

$$k'_1 = \sqrt{\frac{15}{5} \frac{\beta_{15}}{\beta_5}} k_4 = 0.027, \quad k'_4 = \sqrt{\frac{13}{5} \frac{\beta_{13}}{\beta_5}} k_4 = 0.023,$$

$$U'_{CC} = \frac{1}{13 \left(\frac{k_3}{k_4}\right)^2 + 15 \left(\frac{k_2}{k_1}\right)^2 + 1} = 0.024,$$

$$U'_{13} = U'_{CC} \left(\frac{k_3}{k_4}\right)^2 = 0.041, \quad U'_{15} = U'_{CC} \left(\frac{k_2}{k_1}\right)^2 = 0.0298,$$

$$Q'_C = \frac{U'_{CC} + 15U'_{15} + 13U'_{13}}{\frac{U'_{CC}}{Q_{CC}} + \frac{15U'_{15}}{Q_{15}} + \frac{13U'_{13}}{Q_{13}}} \approx 9660, \quad \text{and}$$

$$\beta'_C = \frac{Q'_C}{Q_C} \left[\frac{1 + \frac{5U_5}{U_{CC}} + \frac{8U_8}{U_{CC}}}{1 + \frac{15U'_{15}}{U'_{CC}} + \frac{13U'_{13}}{U'_{CC}}} \right] \beta_C = 3.63.$$

The field ratio range should remain unchanged because it depends only on k_2 and k_3 . When the 13- and 15-cell structures became available, the low-power

coupler model was coupled to them and the parameters were remeasured. Remeasured values are compared with scaled values in Table I.

TABLE I
SCALED AND MEASURED PARAMETERS

	Scaled	Measured
k'_{14}	0.027	0.0273
k'_{14}	0.023	0.0223
U'_{cc}	0.024	0.023
U'_{13}	0.041	0.041
U'_{15}	0.0298	0.0272
Q'_{cc}	9,660	11,100
β'_{cc}	3.63	4.86
Range of E_{15}/E_{13}	2.5	2.7

The Q of the center cell (Q_{cc}) was calculated from the above measurements to be $Q_{cc} = 543$. This higher value confirms that the measurement of the center-cell Q gave an underestimate because of the taped slots and would account for the discrepancies between the scaled and measured values of β'_{cc} and Q'_{cc} in Table I.

Mechanical Description

The low-power test model of the coupler was made of aluminum with hand-operated tuners. Movable walls and metal inserts were used to change the aspect ratios of the rectangular cells. All coupling slots were cut in removable plates for ease in making changes.

The high-power coupler is now being fabricated. It will operate under high vacuum, and slots for vacuum pumping are provided in the center cell. Cell tuners will be remotely operated with a position resolution of ~ 0.1 mm. Expansion joints made of one-convolution welded bellows are provided in the coupling cells. These joints should handle any dimensional changes caused by temperature variations without putting undue stress on the other structures that have tight alignment tolerances. The coupler is made of OFHC copper and will be hydrogen brazed. The coupler Q is expected to be in the range of 2000 to 4000.

Three-Post Bridge Coupler

At the suggestion of Jim Potter, a low-power model of a three-post-loaded coupler similar to the LAMPF bridge couplers² was built. The model was not coupled to other structures.

Figure 5 shows a schematic of this model. The coupler consists of a cylindrical cavity loaded by three variable-length rotatable posts with eccentric tabs on their ends. The posts serve to couple the cavity TM_{010} mode at 1.3 GHz with the TM_{011} - and TE_{113} -like modes, whose resonant frequencies were lowered by the insertion of the posts. Figure 6 shows the equivalent three-resonator model of the device. Coupling factor k_3 is large and fixed; whereas, the absolute and relative magnitudes of k_1 and k_2 can be varied by rotation of the eccentric tabs away from a direction perpendicular to the cavity axis. The variation of k_1 and k_2 results in different admixtures of the three modes, giving an end-to-end asymmetry in the cavity fields, as in the rectangular-cavity coupler's center cell. Field perturbation measurements showed a field asymmetry (ratio of fields on one end of the cavity to the fields at the other end) range of 1:1 to 1:1.5.

The relative phases of the fields at the ends of the cavity varied less than 0.1° for the full range of asymmetries.

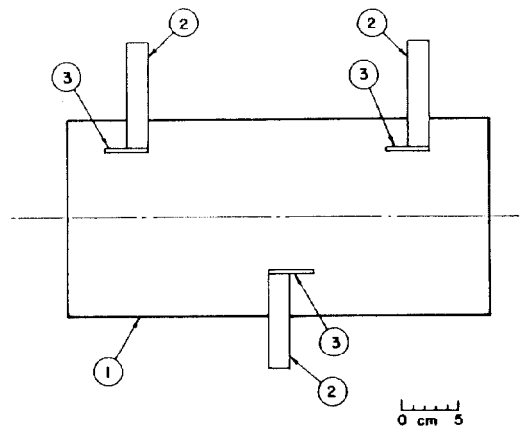


Fig. 5. Three-post bridge coupler: (1) cylindrical cavity, (2) loading posts, and (3) eccentric tabs.

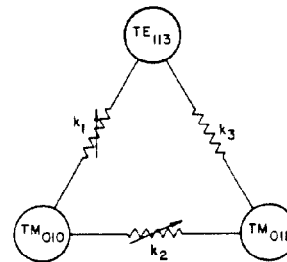


Fig. 6. Three-post bridge coupler equivalent resonator.

Conclusions

The measurements on the rectangular cell coupler show the following:

- The desired range of ratios of accelerator-to-decelerator fields can be achieved while keeping these fields phase-locked to $\sim 1^\circ$.
- The accelerator and decelerator fields remain locked in phase regardless of power-flow direction and cavity Q (that is, they are beam-loading independent).
- Coupling factors, coupled cavity Q s and field amplitudes can be quite well predicted for structures, even when these structures are not available for early tests.
- The waveguide coupling factor (β'_{cc}) is large enough to operate the final system under the expected beam-loading factor (0.74) while recovering only 50% of the beam energy.

We also conclude that, with suitable modifications, the three-post bridge coupler could be used in the FEL energy-recovery experiment.

References

1. J. M. Watson, "Free Electron Lasers and Related Topics," Proc. 1984 Linac Conf., Gesellschaft für Schwerionenforschung, Darmstadt report GSI-84-11 (September 1984), p. 256.
2. J. Potter and E. A. Knapp, "Bridge Coupler Design and Tuning Experience at Los Alamos," in Proc. of the 1972 Proton Linear Accelerator Conf., Los Alamos National Laboratory report LA-5115 (November 1972), p. 250.